Smart Structures and Systems, *Vol. 29, No. 2 (2022) 311-319*
https://doi.org/10.12989/sss.2022.29.2.311

Effect of plastic deformation on the martensitic transformations in TiNi alloy

Fedor S. Belyaev [1a], Margarita E. Evard[*2] and Aleksandr E. Volkov [2b]

[1] *Laboratory of Mathematical Methods in Mechanics of Materials, Institute for Problems in Mechanical Engineering of the RAS, V.O., Bolshoj pr. 61, St. Petersburg, 199178, Russia*
[2] *Chair of Elasticity Theory, Saint Petersburg State University, Universitetskaya Nab. 7-9, St. Petersburg, 199034, Russia*

(*Received July 24, 2021, Revised September 21, 2021, Accepted October 19, 2021*)

Abstract. A model of plastic deformation of the shape memory alloys which describes dislocation slip at the microlevel is developed. A condition similar to the Schmid law was adopted for the determination of dislocation slip onset. A description of the interaction of plastic deformation and martensitic transformations by taking into account the densities of deformation defects is proposed. It is shown that the model can correctly describe the effect of plastic strain on the shape memory effect. The proposed model is also capable of describing the two-way shape memory effect.

Keywords: martensitic transformations; microstructural modelling; plastic deformation; shape memory alloys; TiNi; two-way shape memory

1. Introduction

Shape memory alloys (SMA) are a class of smart materials with the capacity to recover large inelastic deformations due to their unique properties such as shape memory effect, superelasticity, etc. They are widely used in many engineering fields such as aerospace, civil engineering, biomedicine etc. (e.g., Humbeeck 1999, Morgan 2004, Hartl and Lagoudas 2007, Chrysostomou *et al*. 2008, El-Attar *et al*. 2008, El-Borgi *et al*. 2008, Beiraghi 2019, Narjabadifam *et al*. 2020). The unique properties of SMA are based on reversible thermoelastic martensitic transformations; however, at high loads and strains, they can undergo not only reversible phase deformation, but also irreversible plastic deformation. Plastic shear is not only one of deformation mechanisms of a SMA but also plays an important role in the formation of its functional properties. The dislocation slip is responsible for the formation of the two-way shape memory effect and for the "training" of the material. Thus, plastic deformation can be used to purposefully improve of the SMA properties. Therefore, it is difficult to overestimate the importance of taking into account the effect of plastic deformation when creating SMA applications. Unfortunately, it is impossible to describe in a simple way all the features of the influence of this deformation on the SMA functional properties. In this regard, there is a need for specific calculation tools that would make it possible to describe both the plastic deformation itself and its effect on the SMA functional properties.

Many constitutive models have been formulated to describe the SMA deformation. These models can be divided mainly into two groups: macroscopic models and micromechanical ones. Macroscopic models describe deformation phenomenologically based on macroscopic experimental data. These models make it easy to pick material constants. They do not require significant computational resources, and some of them were implemented in a finite element program for performing numerical analysis of SMA parts. Macroscopic models include works (Arghavani *et al*. 2010, Auricchio *et al*. 2007, Bouvet *et al*. 2004, Chatziathanasiou *et al*. 2016, Chemisky *et al*. 2011, Lagoudas and Entchev 2004, Zaki and Moumni 2007, Panico and Brinson 2007, Wang *et al*. 2017, Yu *et al*. 2018a).

However, macroscopic models cannot adequately reflect the microscopic physical nature of the thermomechanical deformation of the SMA. Thus, many micromechanical constitutive models have been developed to describe the mechanical behavior of SMFs, referring to the microscopic physical nature of deformation. In micromechanical models, deformation is considered at the micro level as a set of elementary processes occurring according to one or another deformation mechanism. Using averaging operators, finite element methods, or homogenization methods (for example, the self-consistent method), the constitutive model of a single crystal can be extended to a polycrystalline version, which makes it possible to take into account the real structure of the material. Typical micromechanical models include works (Likhachev 1995, Patoor *et al*. 1996, Volkov *et al*. 1996, Gao *et al*. 2000, Huang *et al*. 2000, Sun and Lexcellent 1996, Evard and Volkov 1999, Volkov and Casciati 2001, Evard *et al*. 2006, Manchiraju and Anderson 2010, Thamburaja 2005, Patoor *et al*. 2006, Long *et al*. 2017, Peng *et al*. 2008, Yu *et al*. 2012, 2018b). The main advantage of such modeling is a higher predictive power than with the macroscopic approach.

*Corresponding author, Ph.D., Associate Professor,
E-mail: m.evard@spbu.ru
[a] Ph.D., Senior Researcher, E-mail: belyaev_fs@mail.ru
[b] D.Sci., Professor, E-mail: volkov@math.spbu.ru

ISSN: 1738-1584 (Print), 1738-1991 (Online)

It should be noted that the aforementioned micromechanical constitutive models are mainly focused only on the description of martensitic transformations, reorientation and splitting of twin martensite occurring under thermomechanical actions, and only a few of them describe irreversible plastic deformation. In this study, we will distinguish the irreversible deformation: caused by external forces, which we will call active plastic deformation, and the deformation caused by internal stresses and securing the accommodation of martensite plates, which we will call microplastic deformation. The earliest models describing microplastic deformation were (Sun and Lexcellent 1996, Evard and Volkov 1999, Volkov and Casciati 2001, Evard *et al*. 2006). They introduced internal variables that are measures of microplastic deformations associated with each of the martensite variants. In the work (Sun and Lexcellent 1996), it was assumed that microplastic deformation increases with the motion of the interphase boundaries. In works (Evard and Volkov 1999, Volkov and Casciati 2001, Evard *et al*. 2006), conditions similar to the flow conditions in the one-dimensional case with isotropic hardening were proposed to describe microplastic deformation.

Among others, only a few models describe active plastic deformation associated with dislocation slip (Manchiraju and Anderson 2010, Wang *et al*. 2008, Yu *et al*. 2012). The model (Manchiraju and Anderson 2010) describes the martensite plasticity present only after the austenite–martensite transformation is complete. The model (Wang *et al*. 2008) accounts for both phase transformations and plasticity at the crystallographic level and allows their simultaneous realization. In the work (Yu *et al*. 2012), a model is presented that describes the superelastic behavior of a polycrystalline sample with accounting of active plastic of austenite phase. The works (Yu *et al*. 2013, 2014, 2015) represent the further development of this model and offer descriptions of various deformation mechanisms of the SMA, including microplastic and active plastic deformation. Despite the significant development of microstructural models, they do not describe the effect of active plastic deformation on martensitic transformations.

Previously, the authors developed a model that allows one to describe all the main SMA properties, e.g., shape memory effect, superelasticity, reorientation of martensite, two-way shape memory. It was also used to describe microplastic deformation and its effect on functional properties under cyclic loading (Belyaev *et al*. 2015), to describe the effect of aging on martensitic transformations (Belyaev *et al*. 2019). The addition of the fracture criterion to the model made it possible to describe the fatigue fracture of the SMA under cyclic thermomechanical loading (Belyaev *et al*. 2018). However, despite all the advantages of the developed microstructural approach, it is unable to describe active plastic deformation. In this regard, the aim of this work was to describe active plastic deformation within the framework of the developed microstructural model, as well as the effect of this deformation on phase transformations in SMA.

2. Model

The description of the SMA plastic deformation in this work is based on the authors previously developed model (Belyaev *et al*. 2015, 2018, 2019). In the proposed microstructural approach the strain of SMA representative volume is calculated by describing various deformation mechanisms at the micro-level followed by averaging the strains of micro-volumes. Consideration of different structural levels in the model makes possible accounting for the structure of the material.

2.1 Structural levels and strain averaging

The subject of the description is the representative volume, which is the material point of the specimen. It is considered that the representative volume consists of grains, which in turn consist of domains of austenite and orientation variants of martensite.

Small strain tensors are used. To calculate the strain at the macro-level, the Reuss' hypothesis is applied: the strain ε of the representative volume is found by averaging the strains ε^{gr} of the grains constituting the representative volume. Grains have various orientations ω of the crystallographic axes and averaging is performed over all orientations

$$\varepsilon = \sum_{\omega} f(\omega)\varepsilon^{gr}(\omega), \tag{1}$$

where $f(\omega)$ is the volume fraction of grains with orientation ω. The strain of each grain is found as the sum of micro-strains obtained from various deformation mechanisms

$$\varepsilon^{gr} = \varepsilon^{e} + \varepsilon^{T} + \varepsilon^{Ph} + \varepsilon^{MP} + \varepsilon^{P}. \tag{2}$$

Elastic ε^{e}, thermal ε^{T}, phase ε^{Ph}, microplastic ε^{MP} and active plastic strain ε^{P} are taken into account. Elastic and thermal strains are found in the common way according to Hook's law and the law of thermal expansion. To describe the phase strain, internal variables Φ_n are introduced in the model, such that Φ_n/N is the volume fraction of the *n*-th Bain's variant of martensite in the grain; N is the number of the crystallographically equivalent variants of martensite. The total volume fraction of martensite Φ^{gr} in a grain and the phase strain of the grain ε^{Ph} are calculated as

$$\Phi^{gr} = \frac{1}{N}\sum_{n=1}^{N}\Phi_n, \tag{3}$$

$$\varepsilon^{Ph} = \frac{1}{N}\sum_{n=1}^{N}\Phi_n D^n, \tag{4}$$

where D_n is the tensor of the Bain's deformation for the *n*-th variant of martensite.

2.2 Martensite transformation description

Thermodynamic forces determining the process of the martensitic transformation, i.e., the evolution of the internal variables Φ_n are obtained as derivatives of the Gibbs' potential G. This potential for one grain of the two-phase material can be split into the eigenpotential G^{eig} and the potential of mixing G^{mix}

$$G = G^{eig} + G^{mix}. \tag{5}$$

The eigenpotential is the potential of non-interacting austenite and martensite and is given by relations (see for example Volkov and Casciati 2001)

$$G^{eig} = (1 - \Phi^{gr})G^{A} + \frac{1}{N}\sum_{n=1}^{N} \Phi_n G^{Mn}, \tag{6}$$

$$\begin{aligned} G^{a} = {} & G_0^a - S_0^a(T - T_0) - \frac{c_\sigma^{0a}(T - T_0)^2}{2T_0} \\ & -\varepsilon_{ij}^{0Ta}(T)\sigma_{ij} - \frac{Q_{ijkl}^a \sigma_{ij}\sigma_{kl}}{2}, \\ a = {} & A,\ Mn, \end{aligned} \tag{7}$$

where T_0 is the temperature of the thermodynamic equilibrium of austenite and martensite at zero stress, G_0^a and S_0^a are the values of the Gibbs' potential and of the entropy at $T = T_0$ and $\sigma = 0$, c_σ^a is the specific heat (per unit volume), $\varepsilon^{0a}(T)$ is the strain at $\sigma = 0$, Q^a is the tensor of elastic compliances.

The mixing potential corresponds to the elastic energy of the internal stresses caused by the incompatibilities of the phase deformation. Its correct calculation is a very complicated task demanding the knowledge of the particular configuration of the martensite Bain's domains and plates as well as of the boundary conditions on the internal boundaries. This model exploits the same idea as in (Niclaeys *et al*. 2002) and the mixing potential is approximated by a quadratic form

$$G^{mix} = \frac{\mu}{2}\sum_{m,n=1}^{N} A_{mn}(\Phi_m - b_m)(\Phi_n - b_n). \tag{8}$$

In Eq. (8) new internal variables b_n are introduced. They stand for the oriented deformation defects densities, caused by the internal stresses and reducing the elastic energy of the inter-phase interaction. Material constants μ and A_{mn} describe the magnitude of the interaction as well as the preference of the appearance of the particular combinations of the martensite Bain's variants. An estimation of the values of these constants for TiNi was considered in (Volkov *et al*. 2015). From Eqs. (5)-(8) the thermodynamic forces for the martensitic transformation are derived as

$$\begin{aligned} F_n = -\frac{\partial G}{\partial \Phi_n} \approx {} & \frac{q_0(T - T_0)}{T_0} + D_{ij}^n \sigma_{ij} \\ & -\mu\sum_{m=1}^{N} A_{mn}(\Phi_m - b_m), \end{aligned} \tag{9}$$

were q_0 is latent heat (enthalpy) of the direct martensitic transformation.

In the terms of the thermodynamic forces F_n the condition of the transformation of austenite into the n-th variant of martensite can be formulated as

$$F_n = \pm F^{fr}, \tag{10}$$

where F^{fr} is the dissipative force describing the hysteresis of the martensitic transformation (the deviation of the force F_n from the thermodynamic equilibrium $F_n = 0$); the plus sign in Eq. (10) is for the direct and minus is for the reverse transformation.

2.3 Microplastic deformation description

Microplastic strains are caused by the incompatibility of the phase deformation. The main assumption for its calculation is that the phase strain of a Bain's variant activates a combination of slips producing a strain proportional to the deviator of the phase strain. Thus, the microplastic strain can be calculated as follows

$$\varepsilon^{gr\,MP} = \frac{1}{N}\sum_{n=1}^{N} \kappa \varepsilon_n^{mp} dev(D^n), \tag{11}$$

where ε_n^{mp} are microplastic strains related to the n-th variant of martensite, κ is scaling factor for microplastic strain.

To find the variation of microplastic strains ε_n^{mp} we formulate the flow conditions in the form

$$\left|F_n^p - F_n^\rho\right| = F^y, \quad \left(F_n^p - F_n^\rho\right)dF_n^p > 0, \tag{12}$$

where F_n^p is the generalized force conjugated with the parameters b_n

$$F_n^p = -\frac{\partial G}{\partial b_n} = \mu\sum_{m=1}^{N} A_{mn}(\Phi_m - b_m). \tag{13}$$

The forces F^y and F_n^p are responsible for isotropic and kinematic hardening. The formulated microplastic flow condition is analogous to the classical flow condition in the one-dimensional case. The force F_n^p plays the role of stress and F^y and F_n^p the roles of the flow stress and the back stress respectively.

Deformation defects generated by the micro plastic flow we divide in two groups: oriented defects b_n generating long-range stress fields and scattered defects f, suggesting the evolution equations for them in the form

$$\dot{b}_n = \dot{\varepsilon}_n^{mp} - \frac{1}{\beta^*}|b_n|\dot{\varepsilon}_n^{mp} H\left(b_n \dot{\varepsilon}_n^{mp}\right), \tag{14}$$

$$\dot{f} = \sum_{m=1}^{N}\left|\dot{\varepsilon}_m^{mp}\right| + r_1(f - f_0)\dot{\Phi}_{gr} H\left(-\dot{\Phi}_{gr}\right), \tag{15}$$

where β^* is maximum value of the oriented defects density, r_1 is scattered defects healing factor, f_0 is initial

value of scattered defects, H is the Heaviside function.

For the closing equations that connect the density of deformation defects with hardening the simplest linear form is chosen

$$F_n^{\rho} = a_{\rho} b_n, \tag{16}$$

$$F^{y} = a_y f, \tag{17}$$

where a_{ρ} and a_y are the kinematic and isotropic hardening factors.

2.4 Plastic deformation description

To describe active plastic deformation within the framework of a microstructural model, it is necessary to formulate the constitutive relations of this process at the micro level – for a single grain. As a rule, in metals and alloys, dislocation slip occurs only on several specific crystallographic planes. For other systems, the realization of plastic shears is difficult because of the yield stress for these planes is greater than the ultimate strength of the material.

Any slip plane can be attributed to one of families, each consisting of K_m crystallographically equivalent planes, numbered 1, ..., k, ..., K_m. For example, in the austenitic B2 phase of TiNi SMA slip occurs on the planes belonging to two families: {110} and {100}, first consisting of 6 and the second of 3 planes. Plastic deformation $\varepsilon_{\omega}^{gr\,p}$ in grain ω is the sum of deformations in each of the shear planes belonging to this grain

$$\dot{\varepsilon}_{\omega}^{gr\,p} = \sum_{m=1}^{M} \sum_{k=1}^{Km} \dot{\varepsilon}_{\omega}^{p(m,k)}, \tag{18}$$

where $\varepsilon_{\omega}^{p(m,k)}$ is the deformation carried out by shear in the k-th plane from the m-th family.

In each slip plane we introduce a local basis, such that its 3-d axis is normal to the plane and the 1-st and the 2-nd axes lie in the plane. We assume that the only components of the stress related to this local basis, which produce slip on this plane are $\tau_{31}^{(m,k)}$ and $\tau_{32}^{(m,k)}$. Let σ^{gr} be the effective stress applied to the grain. Then, in consistence with the Reuss' hypothesis these two components are found by the formulae

$$\begin{aligned} \tau_{31}^{(m,k)} &= A_{p3}^{(m,k)} A_{q1}^{(m,k)} \sigma_{pq}^{gr}, \\ \tau_{32}^{(m,k)} &= A_{p3}^{(m,k)} A_{q2}^{(m,k)} \sigma_{pq}^{gr}, \end{aligned} \tag{19}$$

where A_{pq} is the rotation matrix that transforms the crystallophysic basis of the grain ω into the local basis associated with the plane (m,k).

The condition for the onset of the plastic shear is formulated as the Schmid law: plastic flow begins when the shear component of the stress $\tau_{31}^{(m,k)}$ or $\tau_{32}^{(m,k)}$ reaches a critical value τ^{s} for the given slip system

$$\tau^{s\,(m,k)} = \begin{cases} \tau_{31}^{(m,k)}, & if \quad \tau_{31}^{(m,k)} \geq \tau_{32}^{(m,k)} \\ \tau_{32}^{(m,k)}, & if \quad \tau_{31}^{(m,k)} < \tau_{32}^{(m,k)} \end{cases} \tag{20}$$

In this case, deformation accumulates in the admissible shear direction. The components of shear deformation are $\beta_{31}^{(m,k)}$ and $\beta_{32}^{(m,k)}$ on the plane (m,k).

We assume that the flow stress $\tau^{s(m,k)}$ is the sum of the initial (equilibrium) value $\tau_{eq}^{s(m,k)}$ which is the same for all planes belonging to the given m-th group, and the addition $\tau_{def}^{s(m,k)}$ responsible for the strain hardening

$$\tau^{s(m,k)} = \tau_{eq}^{s(m,k)} + \tau_{def}^{s(m,k)}. \tag{21}$$

To calculate the value of $\tau_{def}^{s(m,k)}$ we assume that the strain hardening coefficient $h(m)$ does not depend on the shear value, thus the $\tau_{def}^{s(m,k)}$ growth rate is

$$\dot{\tau}_{def}^{s(m,k)} = \begin{cases} h\left|\dot{\beta}_{31}^{(m,k)}\right|, & if \ \left|\dot{\beta}_{31}^{(m,k)}\right| > 0 \\ h\left|\dot{\beta}_{32}^{(m,k)}\right|, & if \ \left|\dot{\beta}_{32}^{(m,k)}\right| > 0 \end{cases} \tag{22}$$

The plastic deformation of the grain $\varepsilon_{\omega}^{gr\,p}$ is determined using the summation (18), and the macroscopic plastic deformation ε^{p} is determined by averaging over all the grains of the representative volume.

2.5 Plastic deformation and martensitic transformation interaction

Plastic deformation causes generation of deformation defects, for example dislocations. Pile-ups of these defects generate long-range stress fields in the material and, therefore, they are the sources of internal stresses, which contribute to the effective stress applied to the grain, and thus affect the martensitic transformation. In a similar way, the martensitic transformation is affected by microplastic deformation, which arises due to the incompatibility of deformations near the boundaries of growing martensite plates.

The deformation defects produced by the microplastic deformation are taken into account by the densities of these defects b_n generated by the growth of each of 1, ..., n, ..., N variants of martensite. The influence of the densities b_n on the martensitic transformation is taken into account in the mixing potential (8). Since the physical nature of plastic and microplastic deformations is the same (dislocation shear) and they generate the same defects (ensembles of dislocations), it must be possible to express the densities of the defects associated with the plastic deformation in terms of the densities of the defects associated with the microplastic deformation. Thus, the effect of plastic deformation on the martensitic transformation will be taken into account.

To characterize the deformation defects associated with the plastic deformations $\beta_{31}^{(m,k)}$ and $\beta_{32}^{(m,k)}$ of the (m,k) slip system variables $b_1^{(m,k)}$ and $b_2^{(m,k)}$ are introduced. Evolution equations from (Volkov *et al*. 2015) similar to those for microplastic deformation (14) are used for calculation of their values

$$\dot{b}_1^{(m,k)} = \dot{\beta}_{31}^{a(m,k)} - \frac{\left|b_1^{(m,k)}\right|}{\beta^{*}} \dot{\beta}_{31}^{a(m,k)} H\left(\dot{\beta}_{31}^{a(m,k)} b_1^{(m,k)}\right), \tag{23}$$

$$\dot{b}_2^{(m,k)} = \dot{\beta}_{32}^{a(m,k)} - \frac{\left|b_2^{(m,k)}\right|}{\beta^*}\dot{\beta}_{32}^{a(m,k)} H\left(\dot{\beta}_{32}^{a(m,k)} b_2^{(m,k)}\right), \quad (23)$$

where β^* is the maximum value of the defects density.

Variables $b_1^{(m,k)}$ and $b_2^{(m,k)}$ can be viewed as components of the vector $b^{(m,k)}$ which characterizes defects of (m,k) slip system in the local basis of the shear plane. In this basis $b_3^{(m,k)}$ is always equal to zero since the plastic shear is parallel to the slip plane. Therefore, the tensor of internal stresses generated by deformation defects of slip system (m,k) can be introduced as $b_n^{(m,k)}$ where n is the normal vector to the corresponding slip plane. Since vectors $b^{(m,k)}$ and n are perpendicular to each other than tensor $b_n^{(m,k)}$ is a deviator and it can be expressed in coordinates of Ilyushin's five-dimensional deviatorial space (Ilyushin 1990). Its basis tensor in this study is taken in the form

$$\begin{aligned}
U_1 &= \sqrt{\frac{2}{3}}\left(e_1e_1 - \frac{1}{2}e_2e_2 - \frac{1}{2}e_3e_3\right),\\
U_2 &= \frac{1}{\sqrt{2}}(e_2e_2 - e_3e_3),\\
U_3 &= \frac{1}{\sqrt{2}}(e_1e_2 + e_2e_1),\\
U_4 &= \frac{1}{\sqrt{2}}(e_2e_3 + e_3e_2),\\
U_5 &= \frac{1}{\sqrt{2}}(e_3e_1 + e_1e_3),
\end{aligned} \quad (24)$$

where e_1, e_2, e_3 are the basis vectors of the crystallographic coordinate system of the grain.

Summing up the internal stresses of all slip systems, we obtain tensor B, which we call the effective field of defects. Its coordinates B_i in the basis (24) are as follows

$$B_i = \sum_{m,k}(n^{mk}b^{mk}) : U_i. \quad (25)$$

The effective field of defects determines the internal stresses in the grain generated by active plastic deformation. It also makes it possible to take into account the effect of these stresses on martensitic transformations. The contribution of active plastic deformation defects to the stress fields of microplastic deformation can be obtained by the equation

$$b_n = \sum_i B_i U_i : (dev(D^n))^{-1}. \quad (26)$$

With Eqs. (23)-(26), the contribution of plastic deformation defects to the Gibbs' potential is calculated and, thus, an account of the effect of plastic deformation on the martensitic transformations is made.

3. Simulation results

An equiatomic TiNi alloy was chosen as a model material. This alloy is quite popular and widely used in applications. It is known that the plastic shear in TiNi alloy occurs in two systems of planes: {100} and {110}, see for example (Surikova and Chumlyakov 2000, Chowdhury and Sehitoglu 2017). Therefore, to describe the plastic deformation, it is necessary to choose the constants for both slip systems. Fitted material constants for the model

Table 1 Material constants for TiNi alloy

Material constant	Symbol	Value
Number of martensite variants	N	12
Latent heat of the direct martensitic transformation	q_0	-160 MJ/m^3
Characteristic temperatures	M_f	329 K
	M_s	337 K
	A_s	357 K
	A_f	371 K
Temperature of the thermodynamic equilibrium	T_0	354 K
Micro plastic strain scaling factor	κ	7
Isotropic hardening factor	a_y	2 MPa
Kinematic hardening factor	a_ρ	50 MPa
Maximum value of the defects density	β^*	0.013
Initial value of scattered defects	f_0	5
Scattered defects healing factor	r_1	$8\cdot10^{-5}$
Initial yield stress for {100} slip system	$\tau^{s\,eq}{}_{\{100\}}$	85 MPa
Hardening coefficient for {100} slip system	$h^{\{100\}}$	100 MPa
Initial yield stress for {110} slip system	$\tau^{s\,eq}{}_{\{110\}}$	100 MPa
Hardening coefficient for {110} slip system	$h^{\{110\}}$	3000 MPa

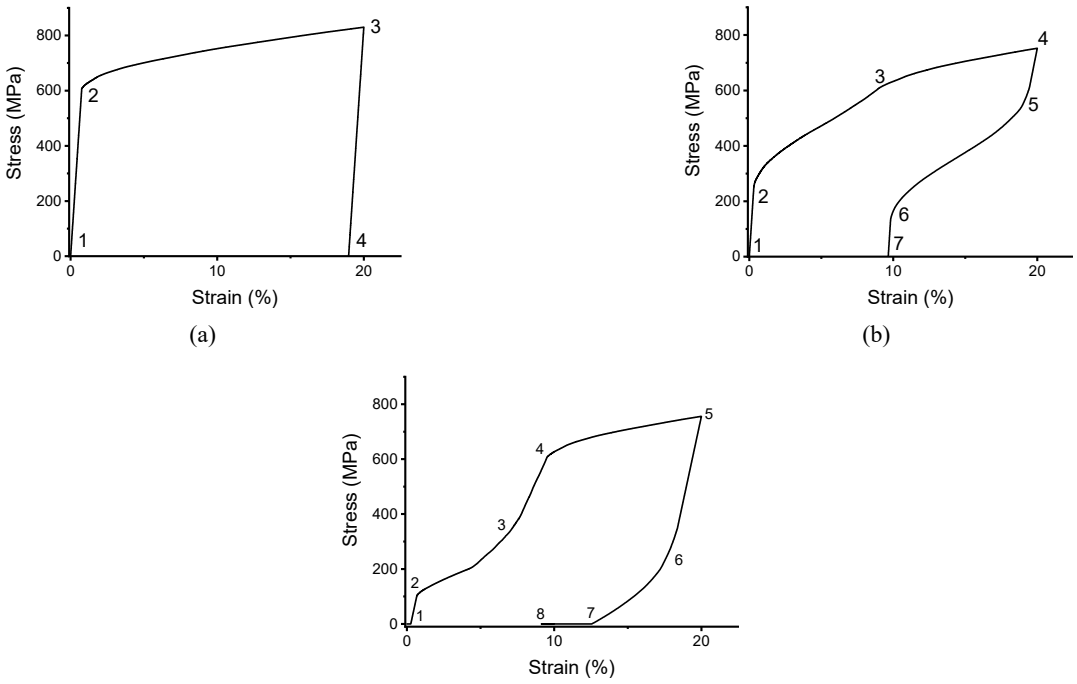

Fig. 1 Deformation curves of TiNi alloy at temperature 600 K (a); 400 K (b); 300 K (c)

material are presented in Table 1.

To test the capabilities of the model in describing the SMA plastic deformation a number of numerical experiments were conducted on the TiNi alloy straining at different temperatures. In order to ensure the implementation of the mechanism of active plastic deformation in each experiment, the straining was carried out up to 20%. This value of strain exceeds the theoretical capabilities of the phase deformation of the TiNi alloy and at the same time does not lead to its fracture. The test temperatures provides different initial states of the alloy: martensite, austenite, high-temperature state when force initiation of martensitic transformations is impossible (also austenite).

The Fig. 1(a) shows the deformation curve of the TiNi alloy at a temperature of 600 K, which is higher than the M_d temperature (i.e., a temperature above which force initiation of the martensitic transformation is impossible). At this temperature, the material is in a high-temperature austenitic state. In segment 1-2, the alloy deforms elastically, at point 2 it reaches the yield point, and then deforms plastically 2-3. Unloading 3-4 occurs according to the elastic law. After unloading, significant residual deformation is observed, since deformation mainly occurred due to the active plastic deformation.

On the Fig. 1(b) the diagram of a TiNi alloy straining at a temperature of 400 K is presented. This temperature is above of the end of the reverse martensite transformation (A_f = 371 K) and below the M_d temperature. At these conditions, the alloy is also in the austenitic state, but there is a possibility of force initiation of the martensitic transformation. In segment 1-2, the alloy deforms elastically. At point 2, a phase transformation begins due to the applied stress and therefore in segment 2-3 the slope of the curve decreases. At point 3, the material reaches the yield limit and in segment 3-4, the mechanism of active plastic deformation acts. Unloading occurs first according to the elastic law in segment 4-5, then in segment 5-6 the reverse martensitic transformation occurs with the recovery of strain (the effect of superelasticity) and elastic unloading continues in segment 6-7. After unloading, a residual strain is observed due to the mechanisms of active plastic and microplastic deformations. The residual strain in this case is less than after straining at a temperature of 600 K because here it is partially restored due to the realization of the superelasticity effect.

On the Fig. 1(c) the diagram of a TiNi alloy straining at a temperature of 300 K is presented. This temperature is lower than the end of the direct martensite transformation (M_f = 329 K). At this temperature, the material is fully in the martensitic state. In segment 1-2 the specimen is deformed elastically. Then at point 2 it reaches the twinning limit and a reorientation of martensite occurs during segment 2-3. At the same time, the volume fractions of martensite variants that provide tensile strain increases due to a decrease in the volume fraction of the other variants. At point 3, the possibilities of material deformation due to the reorientation of martensite are exhausted and in segment 3-4 it is deformed mainly elastically. At point 4, the material reaches the yield limit and in segment 4-5 it deforms plastically. Unloading occurs at first elastically 5-6, and at the end with some reverse reorientation of martensite 6-7. The strain at point 7 is the sum of the phase, active plastic and microplastic strains. In order to separate the strain of the plastic mechanisms, the material is heated to the austenitic state (segment 7-8). After heating, the phase strain is restored (shape memory effect) and at point 8, residual plastic strain is observed. This strain is also less

than in Fig. 1(a), since part of the strain was obtained due to phase transformations.

It is well known that SMA show asymmetry in tensile and compressive deformation properties. The presented model considers the variants of martensite as orientational variants of the Bain's deformation. This make it possible to describe in a natural way the asymmetry of deformation associated with the phase transformations; this is described in detail in Volkov *et al*. (2013). The model in the proposed form cannot describe the asymmetry of active plastic deformation, i.e., the tensile and compressive yield limits will be the same up to a sign. This is due to the use of Schmid's law as a flow condition, since in this case, only the shear components of the stress tensor are taken into account. To take into account the asymmetry of active plastic deformation, it is necessary to use the flow condition that takes into account normal stresses, for example, Prager's law.

To test the capacity of model to describe the effect of plastic strain on the martensitic transformations the shape memory effect following by plastic deformation was simulated and results were compared with experiment. The experimental data for TiNi alloy were taken from work (Belyaev *et al*. 2006) where a number of experiments were conducted according to the scheme shown on the Fig. 2. Straining of the sample in the austenitic state (segment 1-2) was carried out at 600 K, so that only the active plastic deformation was active. Plastic deformation was taken in the torsion mode and the residual strain after unloading 2-3 varied within 2-30%. After plastic deformation the sample was transformed into the martensitic state 3-4 by cooling down to the room temperature, then deformed 4-5 and unloaded 5-6 in such a way that the residual strain γ_r reached the value of 3%. Subsequent heating 6-7 and cooling 7-8 of the sample allowed measuring the strain recovery. Using the developed model, similar numerical experiments were conducted.

The capacity of the body to recover the strain on heating was characterized by the factor of strain recovery K equal to the ratio of the recovered strain to the strain imparted to the body in the martensitic state: $K = \left(\frac{\gamma_{sm}}{\gamma_r}\right)$ where γ_{sm} is the shape memory effect strain. The simulated and experimental dependences of K versus the value of the preliminary plastic strain are presented on the Fig. 3.

The Fig. 3 shows that the strain recovery factor K decreases with preliminary plastic strain growth. As noted in work (Belyaev *et al*. 2006) a decrease of K is associated with the formation of the effect of two-way shape memory (TWSM) effect during plastic straining of the sample in the high-temperature austenitic state. The TWSM effect on heating gives a strain of the opposite sign to shape memory strain, which is responsible for shape recovery, and thus to a decrease in K. The same conclusions can be drawn from the analysis of model curves. On the Fig. 2 one can see the implementation of TWSM effect as a small loop 7-8-9 during cooling and heating without applied stress. The dependence of the strain value of TWSM on preliminary plastic deformation is shown on the Fig. 4.

In this way it can be concluded that the developed model makes it possible to correctly describe the development of internal stresses that affect martensitic transformations through the calculation of deformation defects of plastic deformation. In addition, the accuracy of the model is confirmed by the capacity to describe the TWSM effect, since its implementation is directly related to the development of certain fields of internal stresses.

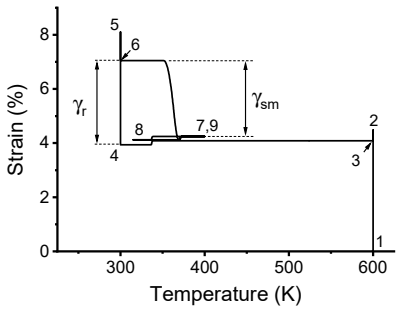

Fig. 2 Experiment scheme on the strain – temperature plane

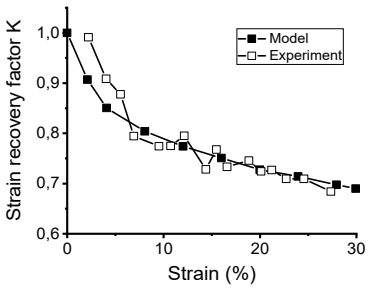

Fig. 3 Strain recovery factor on the value of the preliminary plastic strain

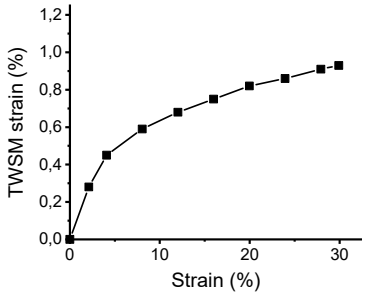

Fig. 4 Two-way shape memory effect strain on the value of the preliminary plastic strain

4. Conclusions

As a result of the present work a model of SMA plastic deformation was developed based on a microstructural approach. Numerical experiments carried out using this model showed:

- Consideration of the shear at the microlevel makes possible describing the plastic deformation of the SMA representative volume.
- Taking into account the densities of the deformation defects produced by active plastic deformation

allows describing its effect on the martensitic transformations. A satisfactory description of the effect the of preliminary plastic strain of the TiNi alloy in austenitic state on the shape memory strain is reached.

- A correct description of the internal stress fields also makes possible describing the effect of two-way shape memory.

Acknowledgments

The reported study was funded by RFBR, projects 19-31-60035 and 19-01-00685.

References

Arghavani, J., Auricchio, F., Naghdabadi, R., Reali, A. and Sohrabpour, S. (2010), "A 3-D phenomenological constitutive model for shape memory alloys under multiaxial loadings", *Int. J. Plast.*, **26,** 976-991. https://doi.org/10.1016/j.ijplas.2009.12.003

Auricchio, F., Reali, A. and Stefanelli, U. (2007), "A three-dimensional model describing stress-induced solid phase transformation with permanent inelasticity", *Int. J. Plast.*, **23**, 207-226. https://doi.org/10.1016/j.ijplas.2006.02.012

Beiraghi, H. (2019), "Earthquake effect on the concrete walls with shape memory alloy reinforcement", *Smart Struct. Syst.*, *Int. J.*, **24**(4), 491-506. https://doi.org/10.12989/sss.2019.24.4.491

Belyaev, S.P., Resnina, N.N. and Volkov, A.E. (2006), "Influence of irreversible plastic deformation on the martensitic transformation and shape memory effect in TiNi alloy", *Materials Science and Engineering*: *A*, **438-440**, 627-629. https://doi.org/10.1016/j.msea.2006.02.067

Belyaev, F.S., Evard, M.E., Volkov, A.E. and Volkova, N.A. (2015), "A microstructural model of SMA with microplastic deformation and defects accumulation: application to thermocyclic loading", *Mater. Today*: *Proceedings*, **2**(suppl. 3), S583-S587. https://doi.org/10.1016/j.matpr.2015.07.352

Belyaev, F.S., Volkov, A.E. and Evard, M.E. (2018), "Microstructural modeling of fatigue fracture of shape memory alloys at thermomechanical cyclic loading", *AIP Conference Proceedings*, **1959**, 070003. https://doi.org/10.1063/1.5034678

Beliaev, F.S., Evard, M.E., Ostropiko, E.S., Razov, A.I. and Volkov, A.E. (2019), "Aging Effect on the One-Way and Two-Way Shape Memory in TiNi-Based Alloys", *Shape Memory and Superelasticity*, **5**(3), 218-229. https://doi.org/10.1007/s40830-019-00226-5

Bouvet, C., Calloch, S. and Lexcellent, C. (2004), "A phenomenological model for pseudoelasticity of shape memory alloys under multiaxial proportional and nonproportional loadings", *Eur. J. Mech. A-Solid*, **23**, 37-61. https://doi.org/10.1016/j.euromechsol.2003.09.005

Chatziathanasiou, D., Chemisky, Y., Chatzigeorgiou, G. and Meraghni, F. (2016), "Modeling of coupled phase transformation and reorientation in shape memory alloys under non-proportional thermomechanical loading", *Int. J. Plast.*, **82**, 192-224. https://doi.org/10.1016/j.ijplas.2016.03.005

Chemisky, Y., Duval, A., Patoor, E. and Ben Zineb, T. (2011), "Constitutive model for shape memory alloys including phase transformation, martensitic reorientation and twins accommodation", *Mech. Mater.*, **43**, 361-376. https://doi.org/10.1016/j.mechmat.2011.04.003

Chowdhury, P. and Sehitoglu, H. (2017), "A revisit to atomistic rationale for slip in shape memory alloys", *Progress in Mater. Sci.*, **85**, 1-42. https://doi.org/10.1016/j.pmatsci.2016.10.002

Chrysostomou, C.Z., Dernetriou, T. and Stassis, A. (2008), "Health-monitoring and system-identification of an ancient aqueduct", *Smart Struct. Syst.*, *Int. J.*, **4**(2), 183-194. https://doi.org/10.12989/sss.2008.4.2.183

El-Attar, A., Saleh, A., El Habbali, I., Zaghw, A.H. and Osman, A. (2008), "The use of SMA wire dampers to enhance the seismic performance of two historical Islamic minarets", *Smart Struct. Syst.*, *Int. J.*, **4**(2), 221-232. https://doi.org/10.12989/sss.2008.4.2.221

El-Borgi, S., Neifar, M., Jabeur, M.B., Cherif, D. and Smaoui, H. (2008), "Use of copper shape memory alloys in retrofitting historical monuments", *Smart Struct. Syst.*, *Int. J.*, **4**(2), 247-259. https://doi.org/10.12989/sss.2008.4.2.247

Evard, M.E. and Volkov, A.E. (1999), "Modeling of martensite accommodation effect on mechanical behavior of shape memory alloys", *J. Eng. Mater. Technol.*, **121**(1), 102-104. https://doi.org/10.1115/1.2815989

Evard, M.E., Volkov, A.E. and Bobeleva, O.V. (2006), "An approach for modelling fracture of shape memory alloy parts", *Smart Struct. Syst.*, *Int. J.*, **2**(4), 357-363. https://doi.org/10.12989/sss.2006.2.4.357

Gao, X., Huang, M. and Brinson, L.C. (2000), "A multivariant model for SMAs Part 1. Crystallographic issues for single crystal model", *Int. J. Plasticity*, **16**(10-11), 1345-1369. https://doi.org/10.1016/S0749-6419(00)00013-9

Hartl, D.J. and Lagoudas, D.C. (2007), "Aerospace applications of shape memory alloys", *J. Aerospace Eng.*, **221**, 535-552. https://doi.org/10.1243/09544100JAERO211

Huang, M., Gao, X. and Brinson, L.C. (2000), "A multivariant micromechanical model for SMAs, Part 2. Polycrystal model", *Int. J. Plast.*, **16**(10-11), 1371-1390. https://doi.org/10.1016/S0749-6419(00)00014-0

Humbeeck, J.V. (1999), "Non-medical applications of shape memory alloys", *Mater. Sci. Eng. A*, **273**, 134-148. https://doi.org/10.1016/S0921-5093(99)00293-2

Ilyushin, A.A. (1990), *Continuum Mechanics*, Moscow State University, Moscow, Russia. [In Russian]

Lagoudas, D.C. and Entchev, P.B. (2004), "Modeling of transformation-induced plasticity and its effect on the behavior of porous shape memory alloys. Part I: constitutive model for fully dense SMAs", *Mech. Mater.*, **36**, 865-892. https://doi.org/10.1016/j.mechmat.2003.08.006

Likhachev, V.A. (1995), "Structure-analytical theory of martensitic unelasticity", *J. Phys. IV*, **05**(C8), 137-142. https://doi.org/10.1051/jp4:1995816

Long, X., Peng, X., Fu, T., Tang, S. and Hu, N. (2017), "A micro-macro description for pseudoelasticity of NiTi SMAs subjected to nonproportional deformations", *Int. J. Plast.*, **90**, 44-65. https://doi.org/10.1016/j.ijplas.2016.12.003

Manchiraju, S. and Anderson, P.M. (2010), "Coupling between martensitic phase transformations and plasticity: A microstructure-based finite element model", *Int. J. Plasticity*, **26**(10), 1508-1526. https://doi.org/10.1016/j.ijplas.2010.01.009

Morgan, N.B. (2004), "Medical shape memory alloy applications–the market and its products", *Mater. Sci. Eng. A*, **378**, 16-23. https://doi.org/10.1016/j.msea.2003.10.326

Narjabadifam, P., Noori, M., Cardone, D., Eradat, R. and Kiani, M. (2020), "Shape memory alloy (SMA)-based Superelasticity-assisted Slider (SSS): an engineering solution for practical aseismic isolation with advanced materials", *Smart Struct. Syst.*, *Int. J.*, **26**(1), 89-102. https://doi.org/10.12989/sss.2020.26.1.089

Niclaeys, C., Ben Zineb, T., Arbab-Chirani, S. and Patoor, E. (2002), "Determination of the interaction energy in the martensitic state", *Int. J. Plasticity*, **18**(11), 1619-1647.

https://doi.org/10.1016/S0749-6419(02)00032-3

Panico, M. and Brinson, L.C. (2007), "A three-dimensional phenomenological model for martensite reorientation in shape memory alloys", *J. Mech. Phys. Solids*, **55**, 2491-2511. https://doi.org/10.1016/j.jmps.2007.03.010

Patoor, E., Eberhardt, A. and Berveiller, M. (1996), "Micromechanical modelling of superelasticity in shape memory alloys", *J. Phys. IV*, **06**(C1), 277-292. https://doi.org/10.1051/jp4:1996127

Patoor, E., Lagoudas, D.C., Entchev, P.B., Brinson, L.C. and Gao, X. (2006), "Shape memory alloys, Part I: general properties and modeling of single crystals", *Mech. Mater.*, **38**, 391-429. https://doi.org/10.1016/j.mechmat.2005.05.027

Peng, X., Pi, W. and Fan, J. (2008), "A microstructure-based constitutive model for the pseudoelastic behavior of NiTi SMAs", *Int. J. Plast.*, **24**, 966-990. https://doi.org/10.1016/j.ijplas.2007.08.003

Sun, Q.-P. and Lexcellent, C. (1996), "On the unified micromechanics constitutive description of one-way and two-way shape memory effects", *J. Phys. IV*, **06**(C1), 367-375. https://doi.org/10.1051/jp4:1996135

Surikova, N.S. and Chumlyakov, Y.I. (2000), "Mechanisms of plastic deformation of the titanium nickelide single crystals", *Phys. Met. Metallogr.*, **89**(2), 98-107.

Thamburaja, P. (2005), "Constitutive equations for martensitic reorientation and detwinning in shape-memory alloys", *J. Mech. Phys. Solids.*, **53**, 825-856. https://doi.org/10.1016/j.jmps.2004.11.004

Volkov, A.E. and Casciati, F. (2001), "Simulation of dislocation and transformation plasticity in shape memory alloy polycrystals", In: *Shape Memory Alloys. Advances in Modelling and Applications*, (Auricchio, F., Faravelli, L., Magonette, G., Torra, V., Eds.), CIMNE, Barcelona, Spain, pp. 88-104.

Volkov, A.E., Evard, M.E., Kurzeneva, L.N., Likhachev, V.A., Sakharov, V.Y. and Ushakov, V.V. (1996), "Mathematical modeling of martensitic inelasticity and shape memory effects", *J. Tech. Phys.*, **66**(11), 3-34. [In Russian]

Volkov, A.E., Emelyanova, E.V., Evard, M.E. and Volkova, N.A. (2013), "An explanation of phase deformation tension–compression asymmetry of TiNi by means of microstructural modeling", *J. Alloys Compounds*, **577**(S1), S127-S130. https://doi.org/10.1016/j.jallcom.2012.05.131

Volkov, A.E., Belyaev, F.S., Evard, M.E. and Volkova, N.A. (2015), "Model of the evolution of deformation defects and irreversible strain at thermal cycling of stressed TiNi alloy specimen", *Proceedings of the 10th European Symposium on Martensitic Transformations* (*MATEC Web of Conferences*), Volume 33, Article No. 03013. https://doi.org/10.1051/matecconf/20153303013

Wang, X.M., Xu, B.X. and Yue, Z.F. (2008), "Micromechanical modelling of the effect of plastic deformation on the mechanical behaviour in pseudoelastic shape memory alloys", *Int. J. Plast.*, **24**, 1307-1332. https://doi.org/10.1016/j.ijplas.2007.09.006

Wang, J., Moumni, Z. and Zhang W. (2017), "A thermomechanically coupled finite-strain constitutive model for cyclic pseudoelasticity of polycrystalline shape memory alloys", *Int. J. Plast.*, **97**, 194-221. https://doi.org/10.1016/j.ijplas.2017.06.003

Yu, C., Kang, G., Song, D. and Kan, Q. (2012), "Micromechanical constitutive model considering plasticity for super-elastic NiTi shape memory alloy", *Computat. Mater. Sci.*, **56**, 1-5. https://doi.org/10.1016/j.commatsci.2011.12.032

Yu, C., Kang, G., Kan, Q. and Song, D. (2013), "A micromechanical constitutive model based on crystal plasticity for thermo-mechanical cyclic deformation of NiTi shape memory alloys", *Int. J. Plast.*, **44**, 161-191. https://doi.org/10.1016/j.ijplas.2013.01.001

Yu, C., Kang, G. and Kan, Q. (2014), "Crystal plasticity based constitutive model of NiTi shape memory alloy considering different mechanisms of inelastic deformation", *Int. J. Plast.*, **54**, 132-162. https://doi.org/10.1016/j.ijplas.2013.08.012

Yu, C., Kang, G., Song, D. and Kan, Q. (2015), "Effect of martensite reorientation and reorientation-induced plasticity on multiaxial transformation ratchetting of super-elastic NiTi shape memory alloy: New consideration in constitutive model", *Int. J. Plast.*, **67**, 69-101. https://doi.org/10.1016/j.ijplas.2014.10.001

Yu, C., Kang, G. and Kan, Q. (2018a), "An equivalent local constitutive model for grain size dependent deformation of NiTi polycrystalline shape memory alloys", *Int. J. Mech. Sci.*, **138-139**, 34-41. https://doi.org/10.1016/j.ijmecsci.2018.02.001

Yu, C., Kang, G. and Kan, Q. (2018b), "A micromechanical constitutive model for grain size dependent thermo-mechanically coupled inelastic deformation of super-elastic NiTi shape memory alloy", *Int. J. Plast.*, **105** 99-127. https://doi.org/10.1016/j.ijplas.2018.02.005

Zaki, W. and Moumni, Z. (2007), "A three-dimensional model of the thermomechanical behavior of shape memory alloys", *J. Mech. Phys. Solids.*, **55**, 2455-2490. https://doi.org/10.1016/j.jmps.2007.03.012

FC